

Microstructure and thermal stability of ultra fine grained Mg and Mg-Gd alloys prepared by high-pressure torsion

J. Čížek^{1,a}, I. Procházka¹, B. Smola¹, I. Stulíková¹, R. Kužel¹, Z. Matěj¹,
V. Cherkaska¹, R.K. Islamgaliev², O. Kulyasova²

¹Faculty of Mathematics and Physics, Charles University, V Holešovičkách 2 CZ-180 00 Praha 8,
Czech Republic

²Institute of Physics of Advanced Materials, Ufa State Aviation Technical University, Ufa 450 000,
Russia

^ajcizek@mbox.troja.mff.cuni.cz

Keywords: Mg alloys, severe plastic deformation, positron annihilation, defects.

Abstract. Bulk samples of pure Mg and Mg-Gd alloys were prepared by high-pressure torsion (HPT). The HPT made samples exhibit ultra fine grained (UFG) structure with grain size around 100 nm. Results of microstructure investigations of the UFG samples obtained by positron lifetime (PL) spectroscopy, transmission electron microscopy (TEM) and X-ray diffraction (XRD) are presented. In particular, lattice defects introduced by HPT were characterized. The data obtained at atomistic level are compared with macroscopic properties given by microhardness measurements.

Introduction

Mg-Gd alloys represent a promising novel light hardenable material with high creep resistance even at elevated temperatures [1]. Despite the favorable strength and thermal stability, a disadvantage of the Mg-based alloys consists in a low ductility, which is not sufficient for industrial applications. Recently it has been demonstrated that ultra fine grained (UFG) metals with grain size around 100 nm can be produced by high pressure torsion (HPT) [2]. A number of UFG metals exhibit favorable mechanical properties consisting in a combination of a very high strength and a significant ductility. For this reason, it is highly interesting to examine microstructure and physical properties of UFG Mg-based light alloys. Following this purpose, microstructure investigations and defect studies of UFG Mg and UFG Mg-10wt.%Gd alloy were performed in the present work.

Experimental

The specimens of Mg (technical purity) and Mg-10wt.%Gd alloy were investigated. The Mg-10wt.%Gd alloy was prepared from the technical purity Mg by squeeze casting. The as-cast material was subjected to the homogenization annealing at 500°C for 6 hours finished by rapid quenching. In addition, a well annealed high purity Mg (99.95 %) was used as a reference sample. UFG samples were prepared from the as-received technical purity Mg and the homogenized Mg-10wt.%Gd alloy by HPT at room temperature up to the true logarithmic strain $\varepsilon = 7$ under high pressure of 6 GPa [2]. The HPT deformed samples were disk shaped with diameter of 12 mm and thickness of 0.3 mm. A fast-fast spectrometer similar to that described in [3] with timing resolution of 170 ps was employed in the present work. Decomposition of PL spectra into exponential components was performed using a maximum likelihood procedure [4]. The PL measurements were accompanied by theoretical calculations of positron lifetimes using the atomic superposition method (ATSUP) [5].

The work was supported by The Czech Grant Agency (contract 106/01/D049), The Ministry of Education, Youth and Sports of Czech Republics (projects COST OC523.50 and 1K03025), and by DFG.

TEM observations were performed on the JEOL 2000 FX electron microscope operating at 200 kV. XRD studies were carried out with the aid of XRD7 and HZG4(Seifert-FPM) powder diffractometers using Cu K α radiation. The microhardness HV was measured by the Vickers method at load of 100 g applied for 10 s using the LECO M-400-A hardness tester.

Results and Discussion

Coarse-Grained Specimens. The reference high purity Mg sample exhibits a single-component PL spectrum, see Table 1. It agrees reasonably with calculated Mg bulk lifetime $\tau_B = 233.2$ ps. On the other hand, PL spectrum of the as-received Mg consists of two components listed in Table 1. The lifetime τ_1 of the shorter component corresponds to free positrons, while the second one $\tau_2 = 256$ ps comes from positrons trapped at defects. The lifetime τ_2 lies between the Mg bulk lifetime τ_B and the calculated lifetime of positrons trapped at Mg-monovacancy $\tau_v = 296.6$ ps. It is typical for dislocations. Dislocation density $\rho \approx 5 \times 10^{12} \text{ m}^{-2}$ and the mean grain size of about 10 μm were estimated by TEM in this specimen. Thus, positrons are trapped at dislocations introduced into the as-received Mg during casting and shaping. In order to check experimentally this interpretation, one technical purity Mg sample was cold rolled to thickness reduction $\epsilon = 40\%$. The second component in the cold rolled sample has virtually the same lifetime τ_2 (see Table 1), indeed, but significantly higher intensity due to a higher dislocation density. Annealing of the as-received Mg at 280°C for 30 min leads to a complete recovery of dislocations reflected also by a remarkable decrease of microhardness HV (the last column of Table 1). The annealed sample exhibits a single component PL spectrum with lifetime which agrees well with that of the reference specimen.

TEM investigations of the homogenized Mg-10wt.%Gd alloy revealed large coarse grains and a low dislocation density below $\approx 10^{12} \text{ m}^{-2}$. The PL spectrum of this specimen is well fitted by two exponential components given in Table 1. The first component with the lifetime $\tau_1 < \tau_B$ can be attributed to free positrons, while the second one with the lifetime τ_2 comes from positrons trapped at defects. The low dislocation density in the specimen approaches the lower sensitivity limit of PL spectroscopy [6]. Therefore, positrons trapped at dislocations cannot represent a noticeable contribution to PL spectrum. The component represents rather a contribution of positrons trapped in quenched-in excess vacancies "frozen" in the sample due to the rapid quenching. This interpretation is supported by the observed lifetime $\tau_2 \approx 300$ ps, which agrees well with the calculated lifetime of positrons trapped in Mg-monovacancy. As free monovacancies in Mg are mobile already below room temperature [7], the observed defects represent vacancies bound to Gd atoms. Enhanced amount of Gd in the vicinity of vacancies was proved by coincidence Doppler broadening measurements [8].

Table 1. Lifetimes and corresponding relative intensities of the exponential components resolved in PL spectra (except of the source contribution). The PL results for HPT deformed materials correspond to the center of the sample. Microhardness values HV are shown in the last column. In case of HPT deformed samples HV in center and at margin of the sample are given. The errors (one standard deviations) are given in parentheses.

Sample	τ_1 (ps)	I_1 (%)	τ_2 (ps)	I_2 (%)	HV (MPa)
high purity Mg well annealed	227.0(5)	100	-	-	
Mg as-received	204(4)	63(1)	256(1)	37(1)	440(40)
Mg annealed 280°C/30 min	225.3(4)	100	-	-	330(20)
Mg cold rolled	160(10)	14(4)	257(2)	86(4)	
Mg-10wt.%Gd homogenized	220(4)	90.9(6)	301(2)	9.1(7)	680(30)
HPT Mg	188(5)	39(1)	257(3)	61(1)	570(30)-620(30)
HPT Mg-10wt.%Gd	210(3)	34(2)	256(3)	66(2)	1670(40)-2330(40)

HPT Deformed Specimens. A bright-field TEM image and an electron diffraction pattern of the HPT deformed Mg specimen are shown in Fig. 1a. Two different kinds of regions were observed: i)

“deformed regions” with UFG grains (100-300 nm) and a high dislocation density, and ii) “recovered regions” with substantially larger grains ($\approx 1 \mu\text{m}$) and almost free of dislocations. The presence of the “recovered regions” indicates an incomplete dynamic recovery of the microstructure during the HPT processing. The XRD back-reflection pattern is a superposition of isolated spots and continuous diffraction rings, which testifies co-existence of the two kinds of regions. The sample shows a texture of (001) type. No significant broadening of XRD profiles was detected so that the dislocation density should be less than about $1 \times 10^{13} \text{ m}^{-2}$. However, a major contribution to the diffraction peaks comes from the “recovered regions” so that the “deformed regions” cannot be well characterized by XRD. The PL spectrum of the HPT deformed Mg consists of the free positron component and a contribution of positrons trapped at dislocations. The lifetime τ_2 of the latter component agrees well with that found in cold rolled Mg for positrons trapped at dislocations. Hence, we can conclude that positrons are trapped at dislocations inside the “deformed regions”. A typical TEM image of the HPT deformed Mg-10wt.%Gd alloy is shown in Fig. 1b. It shows uniform UFG microstructure with the mean grain size about 100 nm, i.e. no dynamic recovery took place during the HPT processing. The electron diffraction pattern shows high-angle missorientation of neighboring grains. A high density of homogeneously distributed dislocations was observed. It is reflected also by a significant broadening of XRD profiles. A lower broadening of (001) profiles with respect to other peaks indicates dominating presence of $\langle a \rangle$ dislocations with Burgers vector $\vec{b} = 1/3.a.[2\bar{1}\bar{1}0]$. A weak (001) texture was found. The PL spectrum of the HPT deformed Mg-10wt.%Gd alloy consists of two components, see Table 1. The first component with the lifetime τ_1 comes from free positrons. The lifetime τ_2 of the second component corresponds well with the lifetime of positrons trapped at Mg-dislocations. One can see in Table 1 that I_2 is comparable for both HPT deformed samples despite the fact that HPT deformed Mg exhibits remarkably lower dislocation density. This surprising effect might be explained by a smaller specific positron trapping rate for dislocations in Mg-10wt.%Gd alloy, where mainly partial dislocations are present due to a lower stacking fault energy. However, this problem remains still open and requires additional investigations. The microhardness plotted in Fig. 2a increases with the radial distance r from the center to the margin of the specimen. A slight increase of HV with r was found in HPT deformed Mg as well. Similar behavior of HV was observed also in HPT deformed Cu [9] and it seems to be typical for a number of HPT deformed metals. It reflects most probably the increase of strain with r . An increase of dislocation density with r was confirmed by PL spectroscopy, see Fig. 2b. The intensity I_2 increases with r in both HPT deformed samples. The uniform distribution of dislocations

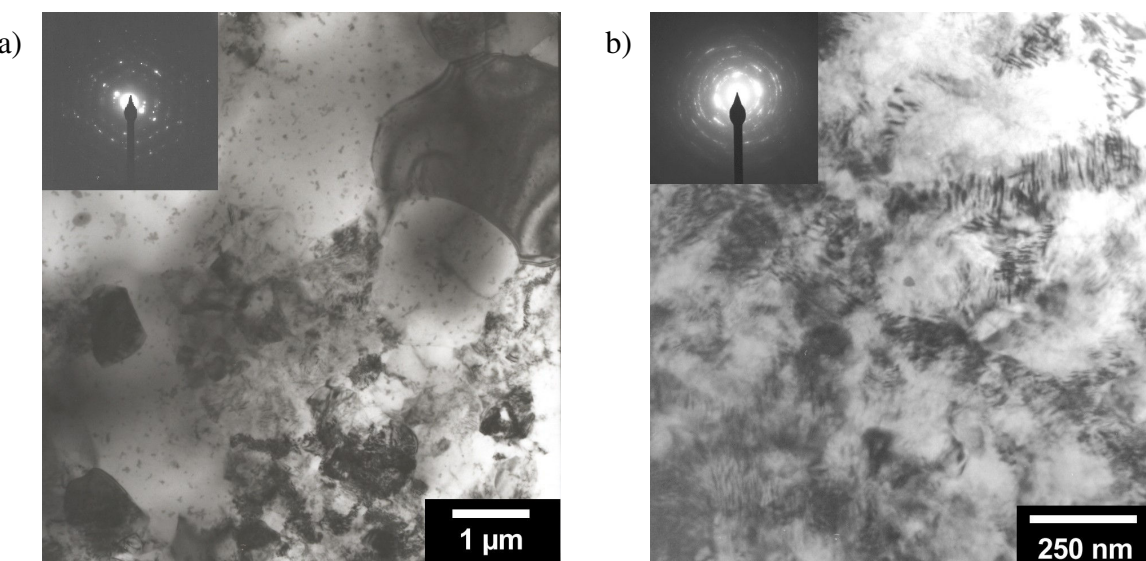


Fig.1: Bright-field TEM image of a) Mg b) Mg-10wt.%Gd alloy deformed by HPT.

and the absence of microvoids represents an important difference compared to HPT deformed Cu [9].

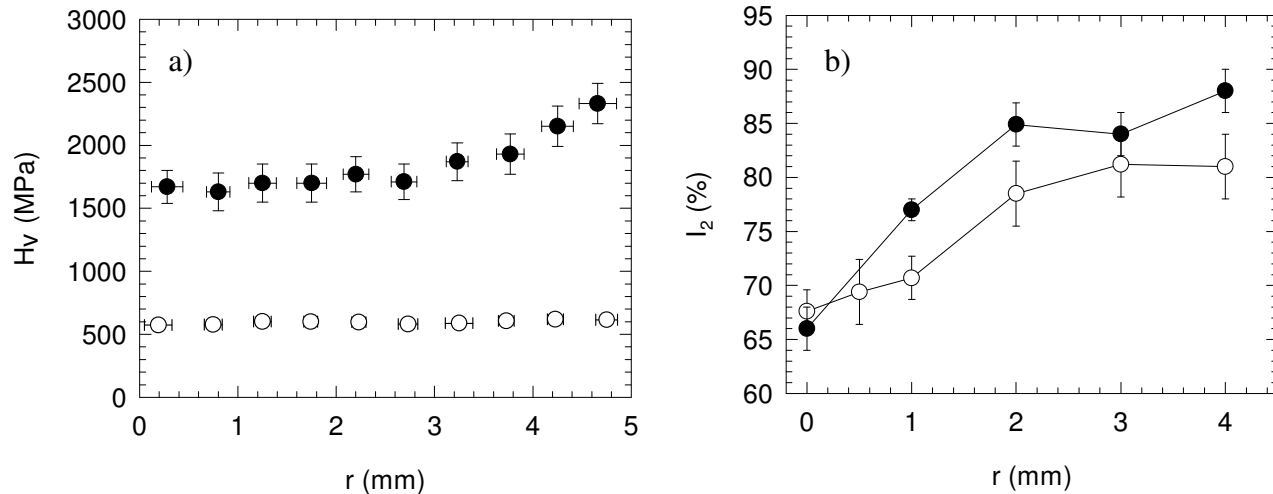


Fig.2: Dependence of a) microhardness b) relative intensity of the PL defect component on the radial distance r from the center of sample. Full circles – HPT deformed Mg-10wt.%Gd, open circles – HPT deformed Mg.

Summary

Microstructure of HPT deformed Mg and Mg-10wt.%Gd was characterized and compared with initial coarse grained materials. An incomplete dynamic recovery took place during HPT processing of Mg sample which resulted in a binomial type of structure. The HPT made Mg-10wt.%Gd exhibits homogeneous UFG microstructure with high density of uniformly distributed dislocations and grain size about 100 nm. No microvoids were found. Both HPT deformed specimens exhibit a significantly increased microhardness compared to initial coarse-grained materials.

References

- [1] P. Vostrý, B. Smola, I. Stulíková, F. von Buch, B.L. Mordike: phys. stat. sol. (a) Vol. 175 (1999), p. 491.
- [2] R.Z. Valiev, R.K. Islamgaliev, I.V. Alexandrov: Prog. Mat. Sci. Vol 45 (2000), p. 103.
- [3] F. Bečvář, J. Čížek, L. Lešťák, I. Novotný, I. Procházka, F. Šebesta, Nucl. Instr. Meth. A Vol. 443 (2000), p. 557.
- [4] I. Procházka, I. Novotný, F. Bečvář, Mat. Sci. Forum Vol. 225-257 (1997), p. 772.
- [5] M.J. Puska, R.N. Nieminen, J. Phys. F: Met. Phys. Vol. 13 (1983), p. 333.
- [6] P. Hautojärvi, C. Corbel, in: Proceedings of the International School of Physics “Enrico Fermi”, Course CXXV, (Ed. A. Dupasquier, A.P. Mills), IOS Press, Varena 1995, p. 491.
- [7] M. Fahnle, B. Meyer, J. Mayer, J.S. Oehrens, G. Bester, in: Diffusion Mechanisms in Crystalline Materials (Ed.: Y. Mishin et al.) MRS Symposia Proceedings No. 527, p. 23.
- [8] J. Čížek, I. Procházka, F. Bečvář, I. Stulíková, B. Smola, R. Kužel, V. Cherkaska, R.K. Islamgaliev, O. Kulyasova, to be submitted.
- [9] J. Čížek, I. Procházka, G. Brauer, W. Anwand, R. Kužel, M. Cieslar, R.K. Islamgaliev, phys. stat. sol. (a) Vol. 195 (2003), p. 335.